Published in **Recent Advances in Computational Mechanics and Simulations - Volume II, I.K. International Publishing House, New Delhi, 2006, pp 1339-1345.**

# Flight Dynamic Simulation of a Multibody Configuration Using an Integrated Euler Solver

**M. Harshavardhan[*], Om Prakash[†], N. Ananthkrishnan[‡]**
[*] Department of Aerospace Engineering, Indian Institute of Technology - Bombay, India–400076. Email: harsha@iitb.ac.in

**Abstract:** A wing-payload system is a two-body flight vehicle with a payload suspended below the wing through a large number of suspension lines. The present study gives a detailed description of 4-DOF longitudinal flight dynamic model of the wing-payload system. The aerodynamic coefficients of the wing are generated using CFD simulations whereas those of the payload are estimated from empirical relations. Using the forces and moments generated on the wing, suspension lines and payload, a dynamic model is developed to study the longitudinal stability characteristics of the system during flight. A detailed analysis of the effect of various parameters on the stability characteristics of the system has also been carried out.

**Keywords:** Flight Dynamic Simulation, Multibody configuration, Euler Solver.

## 1. Introduction

A **Wing-Payload** system is a typical multibody configuration system which consists of the wing with a suspended payload. The large number of suspension lines running down from the lower surface of the wing hold the payload suspended at a specific rigging angle in order to achieve the required glide angle of attack. The wing is the only lifting device of the wing-payload system, whereas the payload (which is essentially a bluff body) contributes to the drag of the system.

Unlike the 6-DOF models used for describing the flight dynamics of a conventional aircraft, the wing-payload system requires a 9-DOF flight dynamic model. The flight dynamics of a wing-payload system is different from that of a conventional aircraft as it is a two-body system. Also, there is relative motion between the wing and the payload. Thus, as developed by Slegers and Costello [1], the wing-payload system can be considered as a two-body system consisting of the wing and payload (each having three rotational degrees of freedom) with a connection point at C (having three translational degrees of freedom). Since the wing-payload system is lightly wing loaded as compared to the aircraft, the apparent mass [2] has a strong effect on the wing flight dynamics and thus has to be included in the flight dynamic model of the wing-payload system.

As the payload is relatively heavier than the wing, the CG of the system is closer to the payload than the wing. Hence, there exists a vertical offset between the wing aerodynamic center and the CG of the system. Thus, the wing drag plays an important role in determining the trim and stability characteristics of the wing-payload system. Another important parameter which affects the trim and stability characteristics of the system is the rigging angle $\mu$ (see Figure 1), defined as the angle between the z-axis of the wing and the link $R_w$. Improper choice of the rigging angle can lead to adverse dynamics during deployment and stall onset at high angles of attack. A stable wing-payload system tends to maintain the angle of attack at which it has been trimmed. Thus, it is essential that autonomous wing-payload systems have adequate trim and stability characteristics.

---

[†] PHD Student, Department of Aerospace Engineering, IIT Bombay; omp@aero.iitb.ac.in
[‡] Associate Professor, Department of Aerospace Engineering, IIT Bombay; akn@aero.iitb.ac.in

Published in **Recent Advances in Computational Mechanics and Simulations - Volume II, I.K. International Publishing House, New Delhi, 2006, pp 1339-1345.**

## 2. Wing-Payload 4-DOF Model

The present study adopts a 4-DOF model obtained from the 9-DOF model presented by Slegers and Costello [1] by limiting the motion of the wing and the payload to the longitudinal direction and dropping the terms arising due to offset of the wing CG from the apparent mass centre.

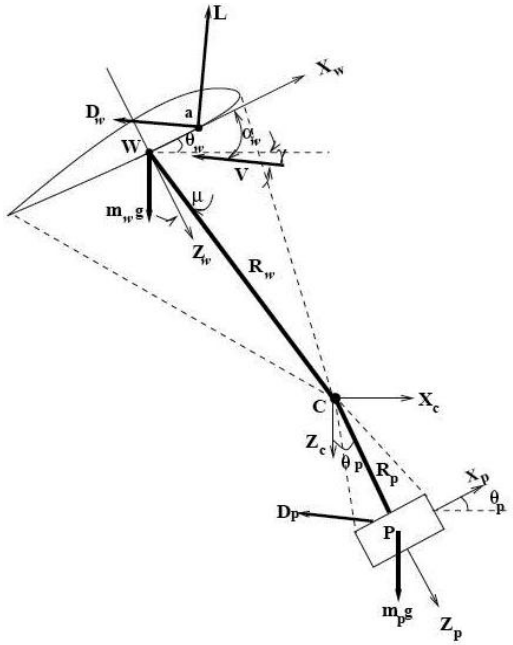


Figure 1: 4-DOF Wing-Payload System

The wing-payload system is modeled as a fixed wing of mass $m_w$ and a payload of mass $m_p$ joined through rigid massless links (having lengths $R_w$ and $R_p$, respectively) connected to the joint C. Both the wing and the payload are free to rotate about the joint C, but are constrained by the internal joint force. As shown in the figure, there are three body-fixed axes: joint C-fixed axis system ($X_c$ axis along the local earth horizontal and $Z_c$ axis normal to the $X_c$ axis pointing downwards), wing body-fixed axis system ($X_w$ axis is along the wing mean chord line and $Z_w$ axis normal to the chord line pointing downwards) and payload body-fixed axis system ($X_p$ axis is normal to the payload link and $Z_p$ axis is along the payload link pointing downwards). It has to be noted that the distance between the wing base line and the wing mean chord line is assumed to be negligibly small. Also, the wing mass centre is assumed to coincide with the wing mid-baseline point and thus, the link $R_w$ joins mid-baseline point to the joint C. Therefore, the rigging angle $\mu$ is defined as the angle between the link $R_w$ and the wing $Z_w$ axis.

### 2.1 Flight Dynamic Model

Longitudinal dynamics of the 4-DOF wing-payload systems are characterized by the horizontal velocity $u_c$ and vertical velocity $w_c$ of the joint C, the pitch angles of wing $\theta_w$ and payload $\theta_p$ (which are the angles made by the $X_w$ and the $X_p$ axis with respect to the horizontal), their respective pitch rates $q_w$ and $q_p$ (rate of change of pitch angles $\theta_w$ and $\theta_p$, respectively), wing angle of attack $\alpha_w$ and flight path angle $\gamma$ [3]. The 4-DOF model of the wing-payload system is formed by deriving the dynamic equations of the wing submodel (consisting of the wing, link $R_w$ and the joint C) and the payload submodel (consisting of the payload, payload link and the joint C) separately. In both submodels, we assume the velocities and the forces at the joint C are common. Considering components of the internal joint forces ($F_x$ and $F_z$) and their moments

Published in **Recent Advances in Computational Mechanics and Simulations - Volume II, I.K. International Publishing House, New Delhi, 2006, pp 1339-1345.**

about the wing CG and the payload CG respectively, the resulting 4-DOF flight dynamic equations appear as below [3]:

$$\begin{pmatrix} m_p\cos\theta_p & -m_p\sin\theta_p & m_pR_p & 0 & \cos\theta_p & -\sin\theta_p \\ m_p\sin\theta_p & m_p\cos\theta_p & 0 & 0 & \sin\theta_p & \cos\theta_p \\ 0 & 0 & I_p & 0 & -R_p\cos\theta_p & R_p\sin\theta_p \\ m_{wA}\cos\theta_w & -m_{wA}\sin\theta_w & 0 & m_{wA}R_w\cos\mu & -\cos\theta_w & \sin\theta_w \\ m_{wC}\cos\theta_w & m_{wC}\cos\theta_w & 0 & -m_{wC}R_w\sin\mu & -\sin\theta_w & -\cos\theta_w \\ 0 & 0 & 0 & I_{wF} & z_{Cw} & -x_{Cw} \end{pmatrix} \begin{pmatrix} \dot{u}_C \\ \dot{w}_C \\ \dot{q}_p \\ \dot{q}_w \\ F_x \\ F_z \end{pmatrix} = \begin{Bmatrix} b_1 \\ b_2 \\ b_3 \\ b_4 \\ b_5 \\ b_6 \end{Bmatrix} \quad (1)$$

where, $Z_{Cw} = R_w(\cos\theta_w + \cos\mu)$, $X_{Cw} = R_w(\sin\theta_w + \cos\mu)$ and

$$\begin{aligned} b_1 &= -m_p g\sin\theta_p - Q_p S_p C_{Dp}\cos\alpha_p \\ b_2 &= m_p g\cos\theta_p - Q_p S_p C_{Dp}\sin\alpha_p + m_p R_p q_p^2 \\ b_3 &= 0 \\ b_4 &= -m_w g\sin\theta_w + Q_w S_w C_x + m_{wC} R_w q_w^2\sin\mu - (C-A)q_w(u_c\sin\theta_w + w_c\cos\theta_w) \\ b_5 &= m_w g\cos\theta_w + Q_w S_w C_z + m_{wA} R_w q_w^2\cos\mu - (C-A)q_w(u_c\cos\theta_w + w_c\sin\theta_w) \\ b_6 &= -X_{wa} Q_w S_w C_z + cQ_w S_w C_M \end{aligned}$$

The kinematic equations for the wing and payload pitch rates are

$$\dot{\theta}_w = q_w$$
$$\dot{\theta}_p = q_p$$

The velocity components of the wing along the $X_w$ and $Z_w$ axis are computed as

$$u_w = u_c\cos\theta_w - w_c\sin\theta_w + R_w\cos\mu q_w$$
$$w_w = w_c\sin\theta_w + w_c\cos\theta_w - R_w\sin\mu q_w$$

The velocity components of the payload along the $X_p$ and $Z_p$ axis are computed as

$$u_p = u_c\cos\theta_p - w_c\sin\theta_p + R_p q_p$$
$$w_p = w_c\sin\theta_p + w_c\cos\theta_p$$

Also, $V_w = \sqrt{(u_w^2 + w_w^2)}$, $V_p = \sqrt{(u_p^2 + w_p^2)}$ and $Q_w = \frac{1}{2}\rho V_w^2$, $Q_p = \frac{1}{2}\rho V_p^2$.

With the apparent mass center of the wing same as its rigid mass center, the total wing moment of inertia becomes $I_{wF} = I_w + I_F$ and the total mass of the wing along the $X_w$ and $Z_w$ axis becomes

$$m_{wA} = m_w + m_{wI} + A$$
$$m_{wC} = m_w + m_{wI} + C$$

The first and the second rows of the matrix are the force equations along the payload axis whereas the fourth and fifth equations of the matrix are the force equations along the wing axis. The third and sixth rows of the matrix are the pitching moment equations of the payload submodel and the wing submodel respectively. All the above equations can be represented as $M\dot{x} = B$ which can be transformed into $\dot{x} = M^{-1}B$, equivalent to a dynamical system $\dot{\mathbf{x}}=\mathbf{f}(\mathbf{x}, \mu)$.

Published in **Recent Advances in Computational Mechanics and Simulations - Volume II, I.K. International Publishing House, New Delhi, 2006, pp 1339-1345.**

### 2.2 Aerodynamic Model

The aerodynamic model of the wing-payload system is:

$$C_L = C_L(\alpha_w)$$
$$C_{Dw} = C_{Dw}(\alpha_w)$$
$$C_{m_{c/4}} = C_{m_{c/4}}(\alpha_w)$$
$$C_{Dp} = 1.05$$
$$C_M = C_{m_{c/4}} + C_{m_{q_w}}(q_w c / 2V_w)$$
$$C_X = C_L \sin\alpha_w - C_{Dw}\cos\alpha_w$$
$$C_Z = -C_L \cos\alpha_w - C_{Dw}\sin\alpha_w$$

The lift and moment coefficients of the wing are computed using an Euler Solver. The Euler solver used in the present study is the LANGLEY Euler Code (*v1.0*) which solves three-dimensional Euler equations on arbitrary multi-block grids and uses the central difference type finite volume approach along with Jameson-Schmidt-Turkel (JST) scheme of artificial dissipation; multistage Runge-Kutta schemes are used to advance in time; implicit residual smoothing and local time stepping are employed as acceleration devices [4]. On the other hand, the drag coefficients of the wing and payload (bluff body) are estimated using empirical relations. Variation of $C_L$, $C_D$ and $C_M$ (at quarter-chord) with Angle of attack ($\alpha_w$) is as shown in Fig 2-4.

### 2.3 Geometric Parameters

Table 1: Wing Payload Geometric Parameters

| Parameter | Value | Parameter | Value |
|---|---|---|---|
| b | 1.1963 m | $m_w$ | 4 kg |
| c | 0.64607 m | $R_w$ | 4.8 m |
| AR | 3.8 | $m_p$ | 35 kg |
| t | 0.1c | $R_p$ | 0.2 m |
| Taper Ratio | 0.562 | $S_w$ | 0.7532 $m^2$ |
| LE Sweep | 30º | $S_p$ | 0.16 $m^2$ |
| TE Sweep | 15.8º | $x_{wa}$ | 0.25c |
| $\Lambda_{25\%}$ | 26.7º | $C_{m_{q_w}}$ | -1.864/rad |

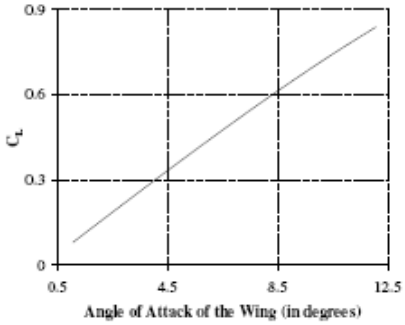

Figure 2: $C_L$ Vs $\alpha_w$

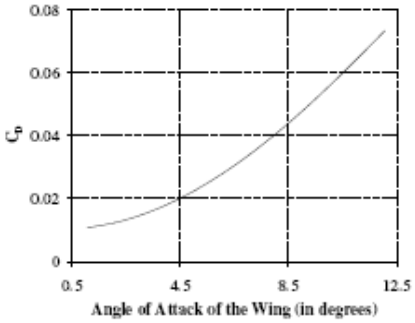

Figure 3: $C_D$ Vs $\alpha_w$

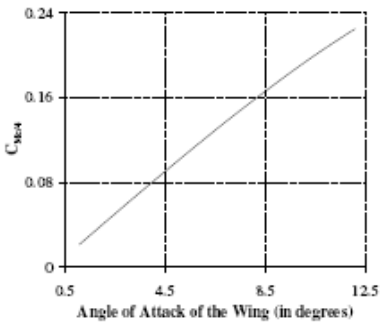

Figure 4: $C_{Mc/4}$ Vs $\alpha_w$

Published in **Recent Advances in Computational Mechanics and Simulations - Volume II, I.K. International Publishing House, New Delhi, 2006, pp 1339-1345.**

Table 1(Contd.): Apparent Mass/Inertia Terms

| | | | |
|---|---|---|---|
| A | $0.913\rho\pi t^2(b/4)$ | $I_F$ | $0.872\rho\ (4c^4b/48\pi)$ |
| C | $0.771\rho\pi t^2(c/4)$ | | |

For the case of our present study, we use an ONERA M6 wing [5] which is a swept, semi-span wing with no twist. The geometric parameters of the wing and payload along with the apparent inertia terms [2] are enlisted in Table 1.

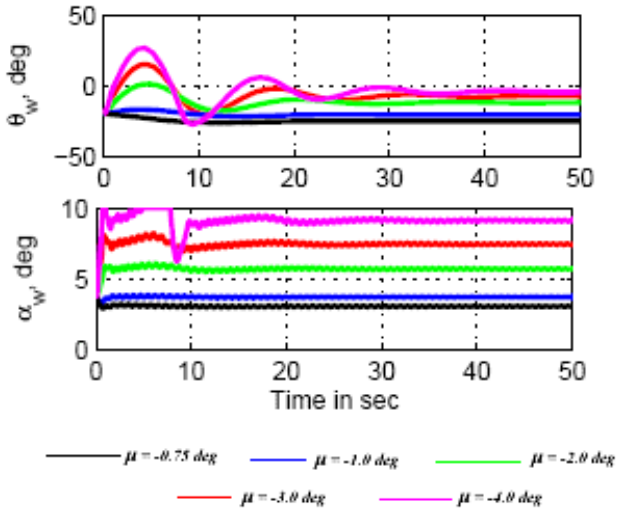


Figure 5

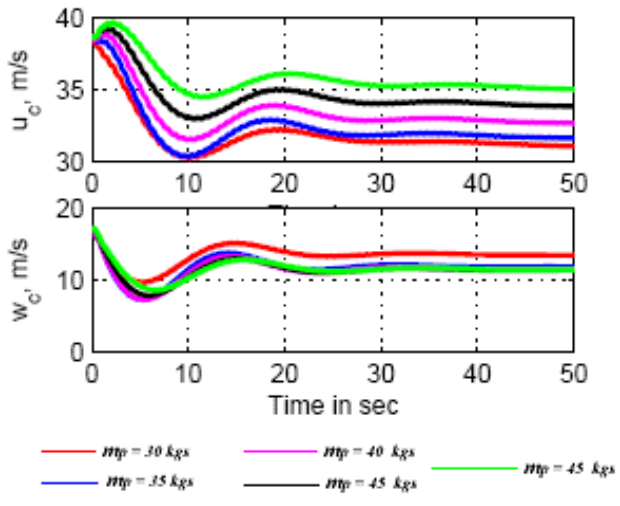


Figure 6

Figure 5: Effect of varying rigging angle (μ) on Angle of Attack ($\alpha_w$) and Pitch Angle ($\theta_w$).
Figure 6: Effect of varying Payload Mass ($m_p$) on Horizontal ($u_c$) and Vertical ($w_c$) Velocities.

### 3. Results and Discussion

Simulation of the 4-DOF flight dynamic model (with pre-specified initial conditions) is carried out for a time interval of 50 seconds. In the present study, there exist initial conditions on the horizontal velocity ($u_c$ = 38.5 m/s), vertical velocity ($w_c$ = 17 m/s), height above ground ($H_i$ = 1000 m), pitch angle of the wing ($\theta_w$ = 20º) and payload pitch angle ($\theta_p$ = 20º). The length of the link $R_w$ is taken to be twice the span of the wing for greater stability. Upon increasing the length of the link $R_w$, the system was found to have improved stability characteristics. For the rigging angle (μ = -1.5º) and payload weight ($m_p$ = 35 kg), the wing-payload system has good trim and stability characteristics. Time histories of the various flight dynamic parameters are plotted for the aforementioned values of μ & $m_p$ in Figure 7 below. As can be inferred from the graphs, the parameters settle down quickly with no huge variations in their values, thus displaying a system with good trim and stability characteristics. The effect of varying rigging angle on angle of attack ($\alpha_w$) and pitch angle ($\theta_w$) of the wing, with payload weight kept constant at 35 kg is shown in Figure 5. The rigging angle is varied between -0.75º and -4.0º; a rigging angle of -4.0º results in a wing angle of attack of approximately 12º which leads to a post-stall condition for the wing. Thus, a safe operating range for the rigging angle would be -0.75º to -3.0º. Figure 6 shows the effect of varying payload mass ($m_p$) on horizontal ($u_c$) and vertical ($w_c$) velocities, this time with the rigging angle kept constant at -1.5º. This particular plot gives the user a precise indication of the velocity at which he would have to fly if he chose a particular payload weight. A variation of payload weight from 30 kg to 50 kg leads to an increase in horizontal velocity and a decrease in vertical velocity.

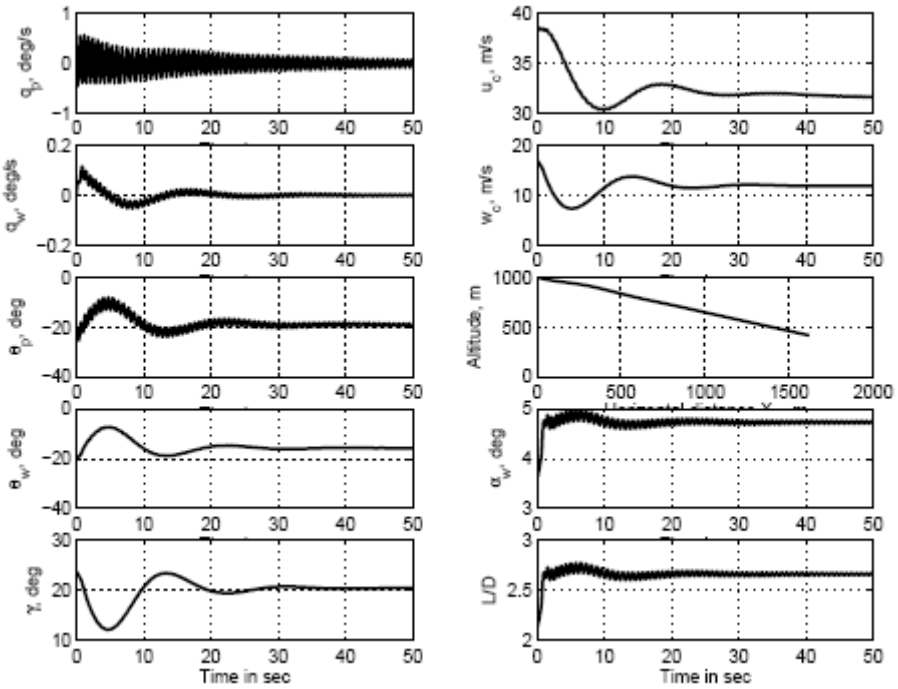


Figure 7: Time histories of the flight dynamic parameters for $\mu$ = -1.5º and $m_p$ = 35 kg

## 3. Conclusions

In the present study, a 4-DOF flight dynamic model was used to determine the trim and stability characteristics for varying system parameters. First, the aerodynamic coefficients of the wing were computed by a CFD program which uses Euler simulations. Drag coefficients of the wing and the payload are estimated from empirical formulas. The 4-DOF model included the effect of apparent mass/inertia terms from literature, thus making the model more accurate. The simulations were run for a time interval of 50 seconds with pre-specified initial conditions. The wing-payload system showed good trim and stability characteristics for a rigging angle ($\mu$ = -1.5º) and payload weight ($m_p$ = 35 kg). The effect of varying rigging angle on $\alpha_w$ and $\theta_w$ with payload mass kept constant; and the effect of varying payload mass on $u_c$ and $w_c$ with rigging angle kept constant has been studied.

## References

1. N. Slegers, M. Costello, 2003, Aspects of Control for a Parafoil and Payload System, Journal of Guidance, Control and Dynamics, 26(6), 898-905.
2. P.B.S. Lissaman, G.J. Brown, 1993, Apparent Mass Effects on Parafoil Dynamics, Proc. 12th AIAA Aerodynamic Decelerator Systems Technology Conference and Seminar, London, UKi, 233-239.
3. Om Prakash, A. Daftary, N. Ananthkrishnan, 2005, Bifurcation Analysis of Parafoil-Payload System Flight Dynamics, AIAA Atmospheric Flight Mechanics Conference and Exhibit, San Francisco, USA, 1-11.
4. A. Jameson, W. Schmidt, A. Turkel, 1981, Numerical Solution of Euler Equations by Finite Volume Method Using Runga-Kutta Time Stepping Scheme, AIAA Paper, 81(1259).
5. V. Schmitt. F. Charpin, 1979, Pressure Distribution on the ONERA M6 Wing at Transonic Mach Numbers, Report of the Fluid Dynamics Panel Working Group 04, AGARD AR138.